

A Study on the Hydrogen Evolving Activity of Electroplated Ni-P Coating by Using the Taguchi Method

Hung-Bin Lee^{1,*}, Chen-Hsiung Hsu² and Dong-Sing Wu^{1,3}

¹Department of Materials Science and Engineering, Da-Yeh University, Changhua 51591, Taiwan, Republic of China

²Department of Mechanical and Automation Engineering, Da-Yeh University, Changhua 51591, Taiwan, Republic of China

³Department of Materials Science and Engineering, National Chung Hsing University, Taichung 40227, Taiwan, Republic of China

Received: January 12, 2011, Accepted: May 18, 2011, Available online: June 27, 2011

Abstract: The optimal catalytic activity of the electrodeposited Ni-P coating with the control of the process parameters was performed in this study by using Taguchi's method. The controlled process parameters included current density, duty cycle and the concentration of the phosphorous acid in the electrolyte. The correlation among the controlled parameters and the resulted hydrogen evolution reaction (HER) activity was discussed with emphasis on the influence of the P content, internal stress, roughness and grain size of the coating. The optimal HER property was obtained for the electrodeposition of Ni-P coating with a phosphorous acid concentration of 5g/l, current density of 16A/dm² and duty cycle of 100 %. The resulted Ni-P coating with a better HER property was the one with P content 3at%, an internal stress higher than 10MPa, grain size 10–15nm and surface roughness higher than 100nm. In addition, the cracking of the coating due to high internal stress favored the raise of the HER activity.

Keywords: Taguchi's method, electrodeposited Ni-P coating, hydrogen evolution rate, phosphorous acid

1. INTRODUCTION

Hydrogen energy is a new clean energy, known as green energy [1]. As there are many process routes in technology to produce hydrogen gas, electrolysis technology is the only method to create hydrogen gas without producing carbon dioxide. However, due to the overpotential in electrolysis, the consumption of electricity in the electrolysis industry is enormous. Therefore, the search for developing a highly catalytic and inexpensive hydrogen evolution electro-catalyst material to reduce energy consumption has an important meaning in theory and technical practice. In literature, nickel-based alloy material was mainly selected as the highly catalytic activity electrode material. De Giz et al used steel as the substrate to produce a Ni-Zn or Ni-Co-Zn alloy in an acidic sulfate and potassium chloride bath. Once the Zn is dissolved by using an alkaline treatment, the surface area can be increased 1000–2000 times [2]. Therefore the reduction of the cathodic deposition potential for hydrogen is one of the methods to produce highly catalytic activity electrode materials. Gala [3] and Conway [4] pro-

duced Ni-Mo-V and Ni-Mo-Cd alloys having a higher hydrogen evolution activity by using the electrodeposition method. However, V and Cd compounds within the bath were toxic, and caused difficult treatment with the waste bath. Hu and Bai used a nickel sulfate system (Watts bath) and mainly applied a direct current for electrodeposition [5]. The Ni-P alloy electroplated layer had a maximum hydrogen evolution rate (HER) with 7 P at% in a 1M NaOH solution. Shervedani used the electrodeposition method to prepare a Ni-P-C_g materials in an alkaline solution, and also achieved higher hydrogen evolution activity [6].

With the research and developments in materials, the use of Ni-P alloy as an electrode material has received high attention. The electrodeposited Ni-P alloy layer has excellent mechanical, corrosion resisting, wear resisting and HER properties [7-14]. There are two reasons that are generally considered for the reduction of hydrogen evolution overpotential; the first is to effectively increase the electrode's surface area (geometric factor), and the second is to reduce the actual hydrogen evolution overpotential (electrochemical factor). In the aspect of effectively increasing the electrode surface area, Shervedani et al considered the high HER

*To whom correspondence should be addressed: Email: lhb6018@mail.dyu.edu.tw

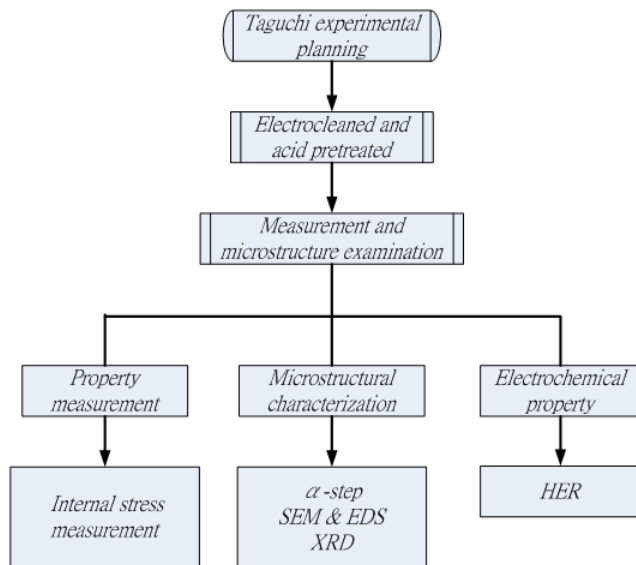


Figure 1. Flowchart of the electrodeposited Ni-P electrocatalytic activity (HER) experiment

in amorphous Ni-P was due to the actual surface area increase, where the maximum HER was NiP₈ in P content 8 at%~30 at% [8]. The electrode surface was porous with high roughness. Panek added Ti powder within a pure Ni electrodeposition solution [9]. Furthermore, when measured in a 5M KOH solution, the electroplated layer with the highest Ti content had the best electrocatalytic activity. Therefore, the reason to cause the HER difference among the electrodes was concluded to be the difference of the surface areas of the electroplated layers. In the aspects with the reduction of the actual hydrogen evolution overpotential, Burchardt et al studied Ni-P HER in an alkaline solution and discovered that between a P content range of 15~27at%, maximum HER occurred when the P content was around 17at% [10]. In addition, HER increases as the thickness of the electroplated layer increased. Krolkowski et al conducted HER measurements in acidic solutions for the electrodeposited layer for P content 7, 20, and 28at% [11]. It was discovered that the crystalline Ni-7P had better HER performance than the amorphous Ni-20P and Ni-28P. Paseka et al showed that the production of the high HER electrode was caused by the amorphous phase in the electroplated layer [12]. Therefore, to obtain excellent HER performance not only depends on the actual area of a surface, but also requires the consideration of whether the structure of the electrode material is amorphous. When P content was 6at%, the Ni-P was amorphous. Furthermore, since the surface of the electrode adsorbed large amounts of hydrogen, the electron structure of the electrodeposited layer changed, and increased HER.

Unlike the general nickel sulfate systems, little research into literature was done for a sulfamate nickel system. Therefore, in order to understand the electrodeposited characteristics and HER performance of the electrodeposited layer, the study used a sulfamate bath to produce a Ni-P layer. The variable factors affecting the electrodeposited Ni-P include the current density, pH value of the bath, and the bath temperature; Lin et al had done detailed discussions regarding these factors [13,14]. In addition, excellent HER

performances for Ni-P HER occurred both in alkaline [5, 6, 8-10, 12] and acidic [11] solutions, however the HER efficiency was low and energy consumption was high in alkaline solutions. Therefore, in this study the Analysis of Variance (ANOVA) and Signal to Noise Ratio (S/N ratio) of the Taguchi Method [15] was used to explore the effect of the electrodeposited Ni-P operation factors toward HER. Moreover, with the effect analysis of the Ni-P process parameters on the electroplated layer structure, a Ni-P which has excellent HER in an acidic environment, and maintains its corrosion resisting performance and high stability was obtained.

2. EXPERIMENTAL METHOD

The experiment conducted a series of systematical approaches by changing the electrodeposited process parameters, using electrochemical measurements, structural analysis and microstructure observations. Taguchi planning used the experimental conditions to produce the electrodeposited Ni-P, and discusses the effect of the electrodeposited process parameters with the HER performance based on the electrochemical measurements. Structural analysis was further conducted to understand the differences within and to find the optimum process condition, as shown in Figure 1.

2.1. Production of electrodeposited Ni-P

In this study, a general phosphorous stripped C1220P copper foil was used as the substrate material with a thickness of 0.3 mm. The anodic material used INCONi blocks (S-Rounds) which had a diameter around 25mm, with thickness of 6mm. The pretreatment steps of the samples were to first cut the substrate copper into a size of 1.5×1.5cm², and first treated with stress relief annealing at a constant temperature of 200C° to remove any residual stress due to the processing of the substrate. In order to control the cleanness and roughness of the sample prior to electrodeposition, the substrate was first grinded with abrasive paper (#240~#1200) to remove oxidation layers on the surface until no stains remained. Further, the samples were placed within a 5% sulfur acid for five minutes for acid pickling and activation, DI water was then used to rinse the surfaces of the samples, then blown with a high-pressure air gun to blow away any liquid on the surface, and then placed within an electrodeposition solution. A sulfamate nickel bath was used for the electrodeposition solution, which was composed of 90 g/l of Ni ions, 0~10 g/l of phosphorous acid, 40 g/l of boric acid, 3 g/l of hydrated nickel chloride, and 2 ml/l of wetting agent; the bath temperature was 50C°. The electrodeposition power was a constant current pulse, which used a precise signal generator (Wave Factory WF1943) to generate the designed wave shapes, and was connected to a current amplifier (NF TA 250) to provide a 0~50A/dm² current density, pulse frequency of 500Hz, and duty cycle of 0~100%. Once the Ni-P was produced, various electrocatalytic tests and analyses of the electrodeposited layer structure were conducted.

2.2. Electrochemical measurements and electroplated layer structure analysis

The experiments with electrochemical measurements used a constant electric potential instrument (EG&G 263A) and a tri-electrode type electrolysis cell, where the working electrode was a Ni-P alloy electrodeposited layer with an exposure area of 1cm²; the counter electrode was a platinum sheet 5 mm wide, 80 mm long, and 0.5 mm thick; the reference electrode was a saturated

calomel electrode (SCE). Before placing within a 0.5 M H₂SO₄ solution and processing cathodic polarization, the oxidation products on the Ni-P surface were first removed by having a constant voltage of -0.6V passed through for 30 minutes. The cathodic polarization curve scan was conducted for electrochemical measuring analysis. The cathodic polarization curve measurement started from 0 V (relative open circuit potential) ~ -0.9 V, with a scanning speed of 1 mV/s.

The measurement for the internal stress of the electrodeposited layer used the flexible-cathode method to perform sample measurements of the open angle, in order to calculate the internal stress value of the electrodeposited layer. The analysis of the electrodeposited layer used an XRD instrument (SHIMADZU XRD-6000) to verify the structure and crystallization characteristics of the Ni-P grain. The Scherrer equation was used to calculate the grain size. An alpha-step profilometer (AMBIOS-Technology XP-2) was used to measure the electrodeposited layer and surface roughness after HER. An SEM (HITACHI S-3000N) was used to observe the electrodeposited layer surface topology.

2.3. The Taguchi Method

The experiment adopted the orthogonal analysis of the Taguchi Method and planned a 3-level and 3-factor, L₉ combination, to find the greatest contributing factor in the HER experiment. The factors had no interactions among each other. According to the literature for the process variables which had a greater effect with the Ni-P electrodeposition process, the three selected experiment factors in this study were the current density, duty cycle, and phosphorous acid concentration. The experiment results further explored the P content, internal stress, surface roughness and the grain size of the electrodeposited layer with the relation to HER. The complete selected Ni-P experiment factors and levels are listed in Table 1. Since there are 3 factors (i.e. phosphorous acid concentration, duty

cycle, and current density) in the experiment system, where each factor had 3 levels (such as pulse duty cycles of 10%, 50%, and 100%); the 3-factor and 3-level L₉ orthogonal array was used to plan the factors and levels according to the L₉ array. The experiment was planned based on a full factorial design to obtain the optimum HER value, in other words, the smaller-the-better analysis method to calculate the Signal to Noise Ratio (S/N ratio) was used to obtain better hydrogen evolution efficiency. The obtained S/N ratios were integrated and discussed by using the response graph and Analysis of Variance (ANOVA), respectively, in order to obtain the largest experimental contributing factor and relative optimized conditions. At the end, a “validation experiment” was performed to verify whether the conclusions through data analysis were correct.

3. RESULTS

3.1. The effect with Ni-P electrodeposited parameters toward HER

Taguchi planning in this study was used to collect the experimental HER characteristics by measuring two specimens with each control variable set, as denoted as Specimen 1 and Specimen 2 in Table 2, using a current density at 100 mA/cm² to measure the overpotential value, η₁₀₀ [15]. The measurement results from the two specimens was employed to check the repeatability of our experiments. Since the purpose of the experiment was to reduce energy consumption and increase HER efficiency, the smaller the better (STB) analysis mainly used the same current density values to obtain lower overpotential values. Therefore, the lower of the η₁₀₀ values, the relative S/N ratio was larger. The S/N ratio (dB) was calculated via STB analysis. In order to obtain the optimum HER combination, the maximum corresponding S/N ratio level of each factor was used. From Figure 2(a), Main Effects Plot for η₁₀₀, and Figure 2(b), Main Effects Plot for S/N Ratios, it was found that the optimum level combination for every factor was factor A3 (current density, 16A/dm²), factor B3 (duty cycle, 100%), and factor C2 (phosphorous acid concentration, 5g/l), that is the 9th group of the previous experiment plan.

The purpose of the analysis of variance (ANOVA) is to use a statistical method to understand the influence levels of the Ni-P process parameters to HER characteristics. The Taguchi experi-

Table 1. Selected factors and levels with the Ni-P experiment

| Factor | Level 1 | Level 2 | Level 3 | units |
|---------------------|---------|---------|---------|-------------------|
| A. Current density | 4 | 8 | 16 | A/dm ² |
| B. Duty cycle | 10 | 50 | 100 | % |
| C. Phosphorous acid | 2 | 5 | 10 | g/l |

Table 2. Experiment planning table

| No | Control Variables | A | B | C | η ₁₀₀ (mV) | | S/N (dB) |
|----|----------------------------------|---|---|---|-----------------------|------------|----------|
| | | | | | Specimen 1 | Specimen 2 | |
| 1 | 2g/l, 4A/dm ² , 10% | 1 | 1 | 1 | -0.676 | -0.682 | 3.36 |
| 2 | 5g/l, 4A/dm ² , 50% | 1 | 2 | 2 | -0.662 | -0.668 | 3.54 |
| 3 | 10g/l, 4A/dm ² , 100% | 1 | 3 | 3 | -0.625 | -0.616 | 4.14 |
| 4 | 5g/l, 8A/dm ² , 10% | 2 | 1 | 2 | -0.639 | -0.633 | 3.93 |
| 5 | 10g/l, 8A/dm ² , 50% | 2 | 2 | 3 | -0.733 | -0.723 | 2.76 |
| 6 | 2g/l, 8A/dm ² , 100% | 2 | 3 | 1 | -0.687 | -0.693 | 3.22 |
| 7 | 10g/l, 16A/dm ² , 10% | 3 | 1 | 3 | -0.645 | -0.651 | 3.77 |
| 8 | 2g/l, 16A/dm ² , 50% | 3 | 2 | 1 | -0.708 | -0.712 | 2.97 |
| 9 | 5g/l, 16A/dm ² , 100% | 3 | 3 | 2 | -0.553 | -0.561 | 5.08 |

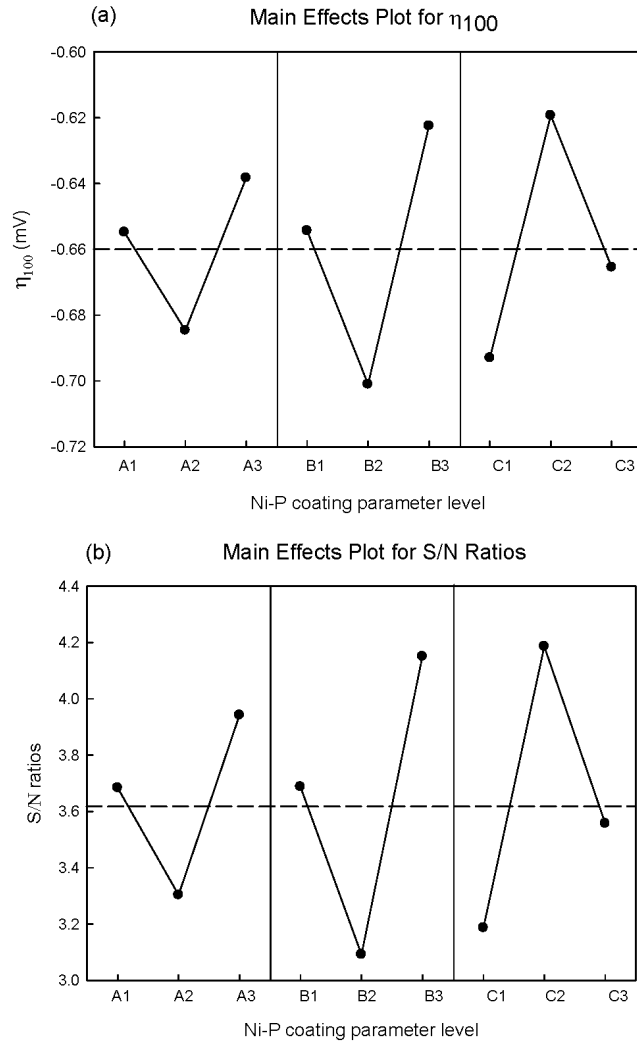


Figure 2. (a) Main effect plot for η_{100} and (b) main effect plot for S/N ratios

ment design version Win 1.12 software was used to perform ANOVA; the experimental results are shown in Table 3. The mean square (MS) is defined as $MS=SS/df$, where SS and df are the sum of squares and degree of freedom. Regarding the statistics test factor, F ratio is the distribution of the degree of freedom $v_1=2$ and

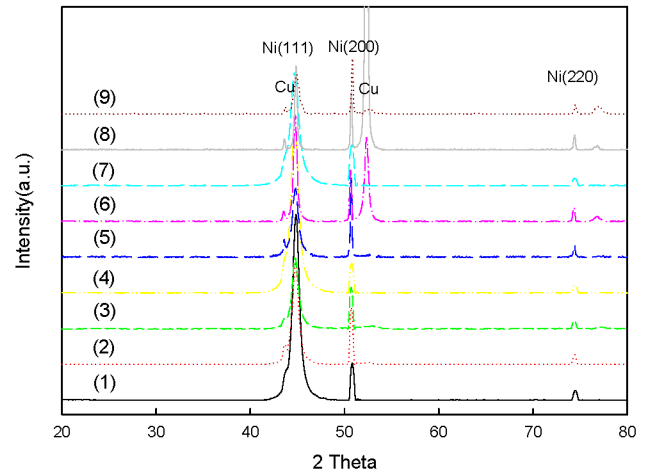


Figure 3. XRD graph for electrodeposited Ni-P

$v_2=2$ (each row consisted by 3 levels, where the degree of freedom for each row was 2, and the overall degree of freedom for L_9 was 8). When the significant level α was 0.05, the specified probability level of F within the table $F_{0.05}(2, 2)=19.00$. The F values of the 3 parameters for factor A, B and C were 7.58, 20.70 and 18.75, respectively. This showed that the three control factors had significant influences regarding HER characteristics. In the aspect of contribution (ρ), the contributions from factor B and C respectively reached 41.01% and 36.96%. The contribution by factor A was 13.70%. From the S/N ratio inspection graph, it could be seen that factors A, B and C were significant factors regarding the influence with HER, with $\rho_{err}=8.33\%$. According to experience, when $\rho_{err}\leq 15\%$, the experiment can be considered to not neglect any important factor.

In order to confirm that the optimum Ni-P process parameters combination confirmed in the experiment is repeatable and of the optimized condition, the sum mode was first applied to calculate the prediction values of the optimum HER parameters level combination. Therefore, within the prediction mode, only the influencing significant factors were considered for optimization of the predicted S/N ratio values of the Ni-P process parameters level combination (A3B3C2), in which each validation experiment was repeated twice. The mean S/N ratio for a 95% confidence interval for HER was 4.99 ± 0.65 [16]. As the mean value of the validation ex-

Table 3. S/N ANOVA analysis table

| Factor | d.f. | SS | MS | F | CNF. LVL% | ρ (%) |
|--------------|------|--------|--------|-------|-----------|------------|
| A | 2 | 0.62 | 0.31 | 7.58 | 88.35 | 13.70 |
| B | 2 | 1.69 | 0.84 | 20.70 | 95.39 | 41.01 |
| C | 2 | 1.53 | 0.77 | 18.75 | 94.94 | 36.96 |
| Error | 2 | 0.08 | - | - | - | - |
| Pooled error | (2) | (0.08) | (0.04) | | | 8.33 |
| Total | 8 | 3.92 | | | | 100.00% |

*Significant parameters ($F_{0.05}(2, 2)=19.00$).

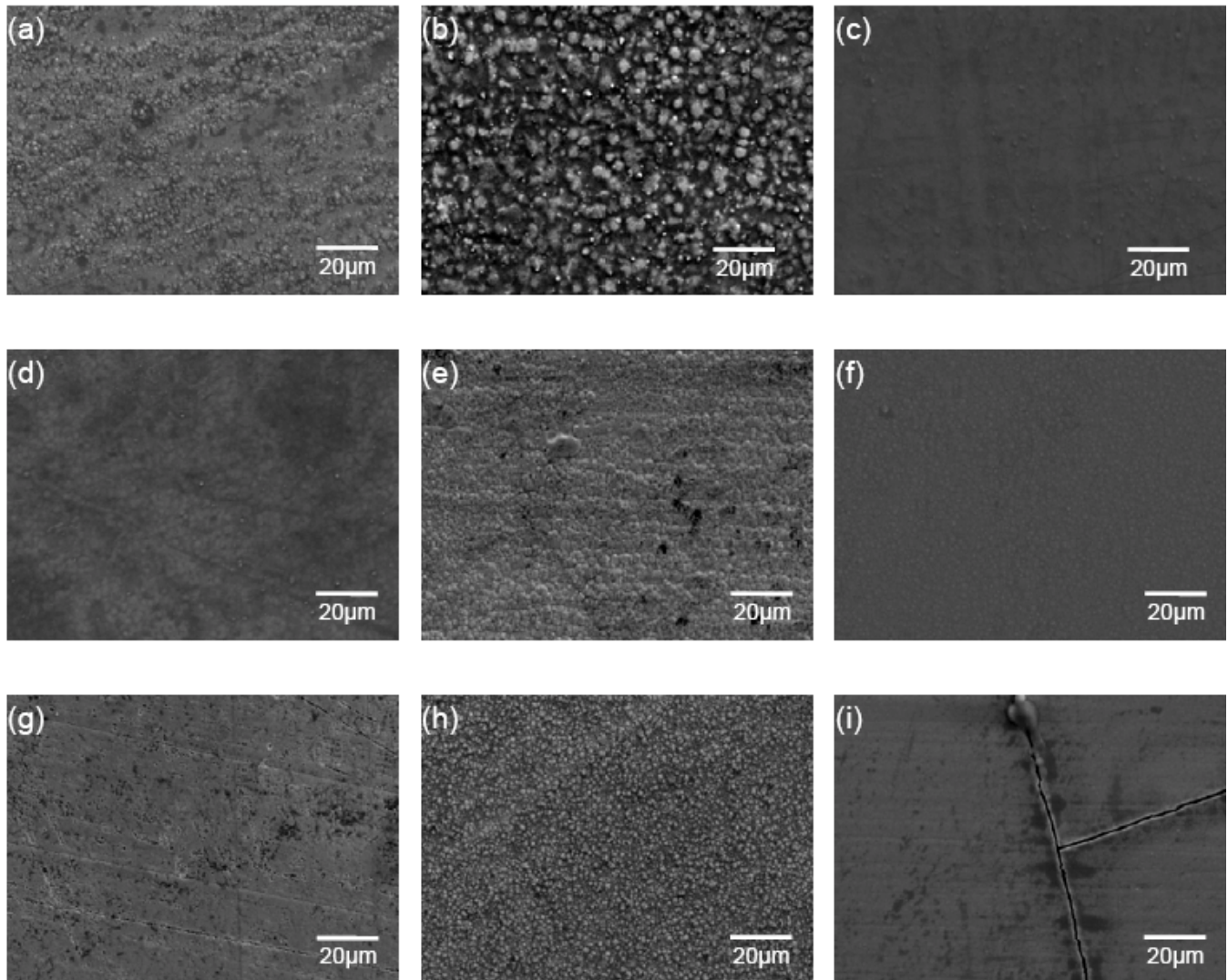


Figure 4. Surface topology of electrodeposited Ni-P as seen through SEM

Table 4. Ni-P electroplated layer for P content, internal stress, roughness, grain size and HER characteristics

| No. | Control Variables | P Content (at%) | internal stress (MPa) | Roughness (nm) | grain size (nm) | η_{100} (mV) |
|-----|----------------------------------|-----------------|-----------------------|----------------|-----------------|-------------------|
| 1 | 2g/l, 4A/dm ² , 10% | 7.66 | -8.8 | 83 | 9.9 | -0.676 |
| 2 | 5g/l, 4A/dm ² , 50% | 8.00 | 9.2 | 112 | 10.4 | -0.662 |
| 3 | 10g/l, 4A/dm ² , 100% | 9.95 | 14.8 | 123 | 10.6 | -0.625 |
| 4 | 5g/l, 8A/dm ² , 10% | 11.75 | -9.3 | 49 | 9.0 | -0.639 |
| 5 | 10g/l, 8A/dm ² , 50% | 9.47 | 7.4 | 114 | 10.9 | -0.733 |
| 6 | 2g/l, 8A/dm ² , 100% | 2.42 | 191.4 | 103 | 19.3 | -0.687 |
| 7 | 10g/l, 16A/dm ² , 10% | 12.57 | -18.5 | 72 | 8.0 | -0.645 |
| 8 | 2g/l, 16A/dm ² , 50% | 2.55 | 164.4 | 97 | 28.3 | -0.708 |
| 9 | 5g/l, 16A/dm ² , 100% | 2.83 | 173.6 | 167 | 13.3 | -0.553 |

periment was 5.08, which lied within the confidence interval range, this indicated that factors A, B and C properly correspond with the corresponding levels. Furthermore, with the determination of the optimal control variables and the confirmation of the repeatability of the experiments, the subsequent and more detail study on the HER activity will be carried out on Specimen 1 only.

3.2. Electroplated layer microstructure, composition, and HER observation

By using XRD to observe the crystallized Ni-P electrodeposited layer, three diffraction peaks (Ni (111), Ni (200) and Ni (220)) were observed, and the electrodeposited layer existed as a crystallized structure form, as shown in Figure 3. The Scherrer equation was used to calculate the grain size at full-width-at-half-maximum, with the results shown in Table 4. The results show that the co-P electrodeposits in the electrodeposited layer would cause the grain structure to miniaturize, and cause the diffraction peaks to become very wide. Among them, when P content ranged between 12.57 at%~2.55 at%, the calculated grain size was between 8.0nm~28.3nm. When it co-existed with the nano-sized Ni grain within the amorphous alloy, this type of structure could adsorb large hydrogen gas amounts, which changed the electron structure of the electrode, and HER was better as the size of the nano grain particles became smaller [10, 17].

On the other hand, the enhancement with the surface area of the electrode material was equivalent to increasing the positions for the adsorption of hydrogen atoms, which can increase the HER reaction rate [8]. The electroplated layer surface topology through SEM observation, according to the experimental sequence of Table 2 and Table 4, are shown in Figure 4. The photos show that the thickness of the electrodeposited layer is around 10 μ m, and the electroplated layer surface has many isle-shaped substances agglomerated to each other and micro holes. The roughness measured by the alpha-step profilometer was between 49nm~167nm. Cracks appeared on the electrodeposited layer surface of Figure 4(i), which was caused by internal stress generated while adsorbing large amounts of hydrogen gas [10].

From the Ni-P cathodic polarization curve (Figure 5), measured within a 0.5M H₂SO₄ solution, the overpotential values η_{100} were between -0.733 V ~ -0.553 V with a measuring current density at 100mA/cm², as shown in Table 4. Whereas in Figure 5, Pt displayed a quite high HER value, showing that when the cathodic current density was quite large, the initial reaction rate at the cathodic interface was quite fast, where the required HER overpotential was quite low. The cathodic current density and voltage appeared to largely increase.

4. DISCUSSION

4.1. Influence of the Ni-P process parameters toward the electrodeposited layer structure

In this study, the current density, pulse duty cycle and phosphorous acid concentration were the main control process factor conditions. As these factors had great influence toward the electrodeposited layer structure, the following is the cross-validation analysis with the P content, internal stress, roughness and grain size. Since the obtained overpotential value, η_{100} , with the two experimental data sets had no large difference, the first data set was used to evaluate the influence of the Ni-P process parameters toward the

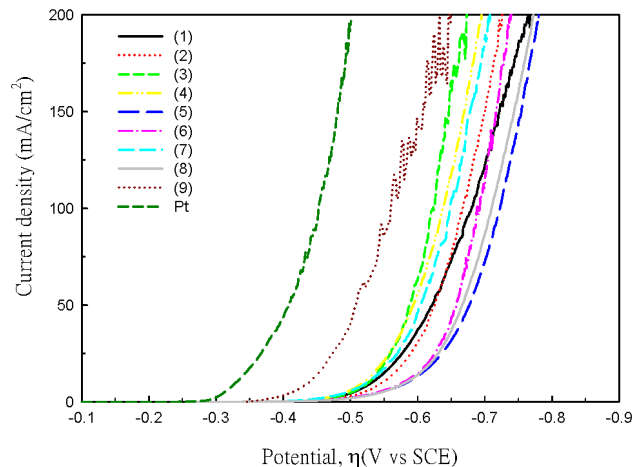


Figure 5. Ni-P cathodic polarization curve under the influence within 0.5M of a H₂SO₄ solution. The number in the legend of each curve indicates the corresponding specimen number listed in Table 2.

electrodeposited layer structure, as shown in Table 4. From the results in Table 4, the data in Figure 6 was obtained. For example, when the phosphorous acid content in Table 4 is 2g/l, the P content point is (7.66+2.42+2.55)/3=4.21, and so on. As shown in Figure 6(a), when the phosphorous acid concentration increased, the P content in the electrodeposited layer increased, and the grain structure became even finer. Besides increasing the phosphorous acid concentration being the main process control factor to increase the P content in the electrodeposited layer, reduction of the duty cycle was also one of the control factors, as shown in Figure 6(b). Since the off period of the pulse electrodeposition may enable the concentration of the metal ions at the interface to maintain its supplement, retaining a high-concentration status, the Ni ions were therefore easily reduced. The co-electrodeposition of P was determined by the induce speed of Ni, and therefore the P content in the electrodeposited layer increased [13, 21]. Table 4(7) shows the P content in the electrodeposited layer was the highest when the pulse duty cycle was 10%, and the phosphorous acid concentration was 10g/l. In addition, the relative miniaturization of the grain in the electrodeposited layer grain and grain size were both minimum among all of the measured values.

As the phosphorous acid concentration of the sulfamate Ni bath system increased, the internal stress of the electrodeposited layer changed from high stress to low stress, as shown in Figure 6(a). When the pulse duty cycle was 100%, the produced Ni-P electrodeposited layer existed in the status of high stress. As the pulse duty cycle was adjusted to 50%, the electrodeposited layer internal stress significantly decreased, as shown in Figure 6(b). The reason for this result was due to the microstructure of the electrodeposited layer, where the grain size had a miniaturization effect as the pulse duty cycle decreased. This caused the interaction forces between the grains during growth to reduce, and decreased the internal stress of the electrodeposited layer. When the pulse duty cycle was 10%, the internal stress of the Ni-P electrodeposited layer mostly existed in the form of compression. The formation of this compress-

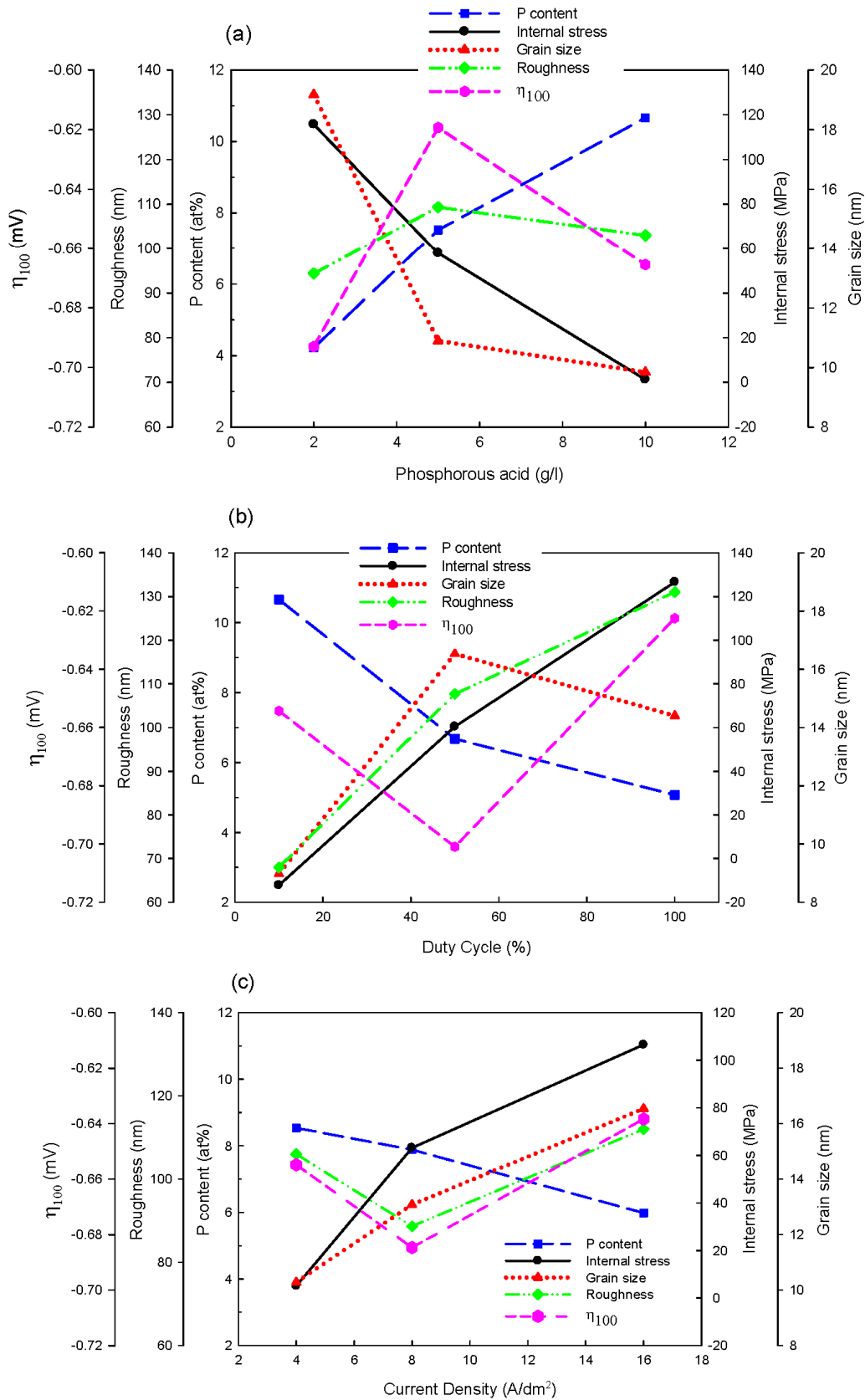


Figure 6. The effects of (a) phosphorous acid, (b) duty cycle, and (c) current density toward the P content, internal stress, surface roughness, grain size and HER of the electrodeposited layer

sive stress caused the production of hydrogen gas during the electrodeposition process, where the hydrogen gas stayed in the inside of the electrodeposited layer or the hydrogen atoms diffused to the grain boundary to form gas bubbles. This resulted in the overall expansion of the electrodeposited layer, where residual compressive stress exists as the bottom material was fixed [13, 22, 23]. The variations of the internal stress of the Ni-P electrodeposited layer varied with the co-electrodeposition amount of P, which caused different microstructure changes. The experiment results showed maximum internal stress when the pulse duty cycle was 100%. As the phosphorous acid content in the bath increased, the grain became finer, and the internal stress of the electrodeposited layer decreased.

The pulse electrodeposited process indeed assisted the internal stress reduction for the Ni-P electrodeposited layer. This showed that only by grain miniaturization or reducing grain growth shall the internal stress of the electrodeposited layer decrease. On the contrary, as shown in Figure 6(c), the increase of the current density and pulse duty cycle accelerated the deposition speed and reduced the electrodeposited layer P content. This caused the internal stress of the electrodeposited layer to enhance. As the electrodeposited layer thickness increased, the internal tensile stress became larger until a critical point is reached, resulting the appearance of cracks on the electrodeposited layer surface, as shown in Figure 4(i). In addition, the surface roughness of the electrodeposited layer plated layer had also relatively increased.

4.2. Correlations between the electrodeposited layer structure and characteristics with HER

From the literature, the summarized factors which affect the HER of the Ni-P electrodeposited layer are the P content, grain size, internal stress and surface roughness of the electrodeposited layer. The following discussed the correlations between the characteristics of the electrodeposited layer and HER characteristics. From Figure 6(a)(b)(c), the results of the HER characteristics and P content of the electrodeposited layer were observed the variation trend is easier to see in graphs than in tables 4 (1)(2)(3). It can be seen that higher HER characteristics (η_{100}) occurred when the P content was near 8 ~ 10at%. Either over high or low P contents would cause a reduction of the HER characteristics. The results had the same trend as the literature [10, 18, 19]. However, with a low P content, sample 9 still had higher HER characteristics (η_{100}). The explanation for this result is as in the previous description (Figure 4(i)), where the over large internal stress of this sample caused cracks in the electrodeposited layer surface. This increased the surface roughness, and might have increased the HER characteristics.

In the aspect of the internal stress effect on the HER value, the results in Figure 6 did not occur in the description in literature, where HER increases with the increasing of the internal stress value, or the electrodeposited layer thickness increased with the internal stress [20]. The presumed reason might be caused by the interaction effect of the other factors such as surface roughness and grain size, and therefore cannot display the effect of the single internal stress factor. This requires variable control in the experiment parameters, where future research can be conducted with the addition in the sample conditions; the experiments have already been carried out. The effect of the electrodeposited layer roughness to-

wards HER characteristics also occurred with similar type issues. This shall require further research in order to be rectified. As for the aspect in the grain size effect, the results in the table significantly indicates an increasing trend of the HER characteristics with the reduction of the grain size. The above result consists of the description in the literature [17], where the amorphous structure surrounds the fine Ni crystallized particles, and smaller grain size can display a better HER performance. The lower HER current density of the sample might be related with the internal stress values. This assumption, however, requires further research.

The optimum control electrodeposited parameters combination obtained by the Taguchi method is given in Table 4(9): with current density 16A/dm², duty cycle 100%, phosphorous acid 5 g/l, the overpotential value resulted as $\eta_{100} = -0.553$ V, P content 2.83 at%, internal stress of the electrodeposited layer 173 MPa, grain size 13.3 nm, surface roughness value 167 nm, and cracks formed on the electrodeposited layer surface. From the experiment data and summarization of the literature, the Ni-P process can control the P content 6~8 at%, internal stress of the electrodeposited layer of 100 MPa or above, grain size of 10~15 nm, surface roughness value greater than 100 nm, and formation of cracks on the electrodeposited layer surface, which assists the in enhancement of the HER characteristics. From this study, the "validation experiment" was conducted to evaluate the 3 factors (current density, duty cycle, and phosphorous acid). The most suitable factor level was set as A3B3C2, and predicted the S/N ratio under optimum conditions was 4.99, where a 95% confidence level considered the expected S/N ratio of the validation experiment range to be 4.99±0.65. This confirmed that the orthogonal array of the Taguchi method greatly reduced the times of experimentation without a loss in reliability. Furthermore, data analysis was conducted by S/N ratio and ANOVA to analyze the effects of the different process parameter factors to achieve the optimum combination. This enables the establishment of the optimum HER of the electrodeposited Ni-P process under minimum experimental costs.

5. CONCLUSIONS

In this study, Taguchi planning was used to seek the optimum electrodeposited Ni-P process parameters for HER. The experiment results analyzed the characteristics of the electrodeposited layer via cross factors with the P content, internal stress, grain size and surface roughness of the electrodeposited layer. When the phosphorous acid concentration increased, current density and pulse duty cycle reduced, the P content of the electrodeposited layer increased, causing the internal stress to decrease, where grain miniaturization shall occur as the P content of the electrodeposited layer increased. When the internal stress increased, the surface roughness also increased, and the electrodeposited layer surface forms isle-shaped agglomerations and cracks. By using the S/N ratio and ANOVA of the Taguchi method, the large contribution and maximum S/N ratio factors were a current density of 16A/dm², duty cycle of 100%, and 5g/l of phosphorous acid. The data was then analyzed to further easily determine the correlations among the P content, internal stress, roughness, and grain size. The resulted Ni-P coating with a better HER property was the one with P content 3at%, an internal stress higher than 10MPa, grain size 10~15nm and surface roughness higher than 100nm. This enables us to reach the goal to obtain experimental process parameters which have small variance.

6. ACKNOWLEDGMENTS

The partial financial support from National Science Council, Taiwan under Grant Nos. NSC 99-2221-E-212-003 and 98-2221-E-027 -083 -MY3 are acknowledged. The Taguchi Method guided by Prof. F. J. Yu, Industrial Engineering & Technology Management, Da-Yeh University, is gratefully acknowledged.

REFERENCES

- [1] W.E. Winsche, K.C. Hoffman, and F.J. Salzano, *Science*, 180, 1325 (1973).
- [2] M.J. De Giz, S.A.S. Machado, L.A. Avaca and E.R. Gonzalez, *J. Appl. Electrochem.*, 22, 973 (1992).
- [3] J. Gala, A. Malachowski and G. Nawrat, *J. Appl. Electrochem.*, 14, 221 (1984).
- [4] B.E. Conway, H. Angerstein-Kozłowska, and M.A. Sattar, *J. Electrochem. Soc.*, 130, 1825 (1993).
- [5] C.-C. Hu and A. Bai, *J. Appl. Electrochem.*, 31, 565 (2001).
- [6] R.K. Shervedani, A.H. Alinoori and A.R. Madram, *J. New Mat. Electrochem. Systems*, 11, 259 (2008).
- [7] H.B. Lee, D.S. Wu, C.Y. Lee and C.S. Lin, *Tribol. Intern.*, 43, 235 (2010).
- [8] R.K. Shervedani and A. Lasia, *Studies of the Hydrogen Evolution Reaction on Ni-P Electrodes*, *J. Electrochem. Soc.*, 144, 511 (1997).
- [9] J. Panek, A. Serek, A. Budniok, E. Rowinski, E. Lagiewka, *Int. J. Hydrogen Energy*, 28, 169 (2003).
- [10] T. Burchardt, *Int. J. Hydrogen Energy*, 25, 627 (2000).
- [11] A. Krolikowski, A. Wiecko, *Electrochim. Acta*, 47, 2065 (2001).
- [12] I. Paseka, *Electrochim. Acta*, 40, 1633 (1995).
- [13] C.S. Lin, C.Y. Lee, F.J. Chen and W.C. Li, *J. Electrochem. Soc.*, 152, 370 (2005).
- [14] C.S. Lin, C.Y. Lee, F.J. Chen, C.T. Chien, P.L. Lin, and W.C. Chung, *J. Electrochem. Soc.*, 153, 387 (2006).
- [15] J. Kubisztal, A. Budniok, A. Lasia, *Int. J. Hydrogen Energy*, 32, 1211 (2007).
- [16] P.J. Ross, *Taguchi techniques for quality engineering*, McGraw-Hill book company, 1996.
- [17] T. Burchardt, V. Hansen, T. VÅland, *Electrochim. Acta*, 46, 2761 (2001).
- [18] A. Krolikowski, A. Wiecko, *Electrochim. Acta*, 47, 2065 (2002).
- [19] C.-C. Hu, A. Bai, *Mat. Chem. Phys.*, 77, 215 (2002).
- [20] I. Paseka, *Electrochim. Acta*, 47, 921 (2001).
- [21] T.M. Harris and Q.D. Dang, *J. Electrochem. Soc.*, 140, 81 (1993).
- [22] T. Burchardt, *Int. J. Hydrogen Energy*, 26, 1193 (2001).
- [23] Y. Tsuru, M. Nomura and F.R. Foulkes, *J. Appl. Electrochem.*, 32, 629 (2002).